JAMSTEC Rep. Res. Dev., Volume 27, September 2018, 109–118
doi: 10.5918/jamstecr.27.109

— Report —

Determination of stable isotope ratios of Ba by ^{130}Ba–^{135}Ba double-spike total evaporation method using thermal ionization mass spectrometry (DS-TEV-TIMS)

Takashi Miyazaki[1*], Jun-Ichi Kimura[1], Shigeyuki Wakaki[2], Bogdan Stefanov Vaglarov[1], and Satoru Haraguchi[1]

An analytical method for determining the stable isotope ratios of Ba was developed by using thermal ionization mass spectrometry (TIMS) and the ^{130}Ba–^{135}Ba double-spike total evaporation method (DS-TEV). We determined the isotope ratios of the ^{130}Ba–^{135}Ba double spike to be ^{134}Ba/^{130}Ba = 0.076623, ^{135}Ba/^{130}Ba = 1.081975, and ^{137}Ba/^{130}Ba = 0.209356 by using the intercept values of the mass-dependent fractionation lines and mixing line.

The measured repeatability of $\delta^{137/134}$Ba of the National Institute of Standards and Technology (NIST) Standard Reference Material (SRM) 3104a was ± 0.018‰ (2SD: 2 standard deviations, n = 7) based on the double-spike total evaporation method using thermal ionization mass spectrometry (DS-TEV-TIMS). The repeatability is comparable to or better than the best repeatability of Ba isotope ratios ever reported.

Keywords : Stable Ba isotope, double spike, total evaporation, TIMS, NIST SRM 3104a

Received 27 February 2018 ; Revised 30 May 2018 ; Accepted 4 June 2018

1 Department of Solid Earth Geochemistry (DSEG), Japan Agency for Marine-Earth Science and Technology (JAMSTEC)
2 Kochi Institute for Core Sample Research (KOCHI), Japan Agency for Marine-Earth Science and Technology (JAMSTEC)

*Corresponding author:
Takashi Miyazaki
Department of Solid Earth Geochemistry, Japan Agency for Marine-Earth Science and Technology
2-15 Natsushima-cho, Yokosuka, Kanagawa 237-0061, Japan
tmiyazaki@jamstec.go.jp

1. Introduction

Ba has seven stable isotopes: ^{130}Ba (0.106% isotope abundance), ^{132}Ba (0.101%), ^{134}Ba (2.417%), ^{135}Ba (6.592%), ^{136}Ba (7.854%), ^{137}Ba (11.232%), and ^{138}Ba (71.698%; de Laeter et al., 2003). Owing to their usefulness as nontraditional stable isotopes with heavy atomic mass, stable isotope ratios of Ba continue to receive attention in various research fields of earth science. The high sensitivity of stable Ba isotope ratios from various geochemical processes such as diffusion, adsorption, dissolution, and precipitation at low temperature has been advantageous in marine geochemical research focusing on the oceanic Ba cycle (Lu et al., 2017, and references therein). The breakthrough study of von Allmen et al. (2010) has dramatically improved the analytical precision of Ba isotope ratios since 2010 (Lu et al., 2017, and references therein). However, a lack of accepted reference materials has created limitations in the analysis of stable Ba isotopes (van Zuilen et al., 2016; Lu et al., 2017), which has led to difficulties in using absolute isotope ratios and interlaboratory data comparisons based on relative isotope ratios such as the δ-notation. Von Allmen et al. (2010) and Miyazaki et al. (2014) suggested the use of $BaCO_3$ issued by International Atomic Energy Agency (IAEA-CO-9) as international reference material. However, this standard is no longer available. Instead, a Ba standard solution issued by the National Institute of Standard and Technology (NIST), SRM 3104a, has recently been proposed as an alternative reference material (van Zuilen et al., 2016). Therefore, precise determination of the Ba isotope ratios of NIST SRM 3104a is required.

Thermal ionization mass spectrometry (TIMS) is a standard technique used for high-precision analysis of stable Ba isotopes, although many laboratories use multiple-collector-inductively coupled plasma-mass spectrometry (MC-ICP-MS). To maximize the advantage of TIMS, the accurate correction of mass-dependent mass fractionation (MDF) occurring in the mass spectrometer is required because internal mass fractionation correction using a canonical stable isotope ratio, which is used in the studies on mass-independent mass fractionation (MIF) especially for the isotope analysis of radiogenic origin, is not applicable for stable isotope analysis.

The double-spike (DS) method is widely used for correction of MDF in Ba isotope analyses (e.g., von Allmen et al., 2010; Miyazaki et al., 2014; van Zuilen et al., 2016). To accomplish high-precision DS-TIMS, sample evaporation from the ion source filament should follow the MDF law, which usually is an exponential law. However, unusual mass fractionation occurs during sample evaporation, most likely owing to isotopically heterogeneous sample domains on the filament (Upadhyay et al., 2008; Andreasen and Sharma, 2009). The total evaporation method (TEV) is useful for overcoming this problem. The influence of unusual mass fractionation can be minimized by the TEV technique, where a sample on the filament completely evaporates and all emitted ion beams are acquired by the collectors (e.g., Suzuki et al., 2004; Fukami et al., 2017, and references therein). During the actual TEV-TIMS analysis, the signal acquisition of a sample is incomplete because of the background noise for which an acquisition threshold is set. In practice, tiny amounts of sample evaporation before and after TEV signal acquisition are not measured owing to the threshold, which results in small error in determination of the isotope ratios. Therefore, additional examination and refinement of MDF are necessary.

In this study, we thoroughly examine and report the DS method in combination with the TEV method (DS-TEV) for analysis of stable Ba isotope ratios. Ba isotope ratios of the NIST SRM 3104a standard using the DS-TEV-TIMS technique are also reported.

2. Experimental

2.1 Reagents, spike, and isotope standard materials

TAMAPURE®-AA grade ultrapure water and TAMAPURE®-AA-10 grade (<10 ppt impurities) 68% HNO_3 (Tama Chemical Co., Ltd., Kawasaki, Japan) were used without additional purification. The TAMAPURE®-AA grade ultra-pure water was used only to dilute the double-spike standard. Deionized water was purified via a two-bottle Teflon® still from Milli-Q® water (Millipore® Molsheim, France). The ^{130}Ba-enriched spike (Batch No. 230901, enrichment 35.84% ± 0.007%, carbonate) and ^{135}Ba-enriched spike (Batch No. 142890, enrichment 93.38% ± 0.02%, carbonate) were obtained from Oak Ridge National Laboratory (ORNL), USA. The ^{130}Ba- and ^{135}Ba-enriched spikes were separately dissolved in 0.5 M HNO_3. Subsequently, the ^{130}Ba and ^{135}Ba spike solutions were mixed and diluted to approximately 1 mg/L. The Ba

reference material (SRM3104a, Ba standard solution (6.994 ± 0.0017 mg/g in 1% nitric acid), Lot No. 140909) from NIST was diluted to 0.01 mg/g using 1% HNO_3.

2.2 Mass spectrometry and data reduction

The Ba isotope ratios were determined by using a Thermo Finnigan TRITON TI® thermal ionization mass spectrometer equipped with nine Faraday cup collectors at the Department of Solid Earth Geochemistry (DSEG), Japan Agency for Marine-Earth Science and Technology (JAMSTEC). An accelerating voltage of 10 kV was used for the Ba isotope analysis. The Faraday collectors were set to simultaneously detect the following isotopes: ^{130}Ba (Low 3), ^{132}Ba (Low 2), ^{134}Ba (Low 1), ^{135}Ba (Center), ^{136}Ba (High 1), ^{137}Ba (High 2), ^{139}La (High 3), and ^{140}Ce (High 4). All Faraday collectors were connected to the amplifiers by using a $10^{11}\Omega$ resistor. The stability of this acquisition system was tested by Miyazaki et al. (2009). The relative efficiencies of the Faraday collectors known, as the cups factors of this TIMS (Miyazaki et al., 2016), were not used in this study because their effect was negligible during the analytical period. Additional cup factor correction should be necessary when the cups are deteriorated (e.g., Miyazaki et al., 2016).

A double Re filament was used as the ion source. Prior to sample loading, both the evaporation and ionization filaments were degassed in a vacuum for 45 min at 4.6 A. Approximately 100 ng Ba was dissolved in 2 μL of 2% HNO_3, and the solution was loaded onto the center of the Re evaporation filament for the standard, double-spike, and mixed samples. A current of 0.6 A was continuously applied during the loading until the solution evaporated.

Using the TRITON TI®, we combined the method files in a sequence file to measure several samples in one sequential run, and we modified the measurement file protocols for Pb isotopes described by Miyazaki et al. (2009). Table 1 shows the four method files included in one sequence file: (1) gain calibration, (2) baseline measurement, (3) filament heating and sample measurement, and (4) blank measurement for baseline drift correction. According to this method, the gain calibration and baseline measurements were conducted prior to heating the filaments. The baseline was measured for 15 min. To monitor the baseline drift during data acquisition, one blank sample measurement was performed at the end of the analytical sequence by measuring the signal intensity of each Faraday collector without heating the ion source filaments. The raw intensity data were used for necessary offline corrections (Miyazaki et al., 2009).

The ionization and evaporation filaments were automatically heated by the filament heating program in the sample measurement method file (Method file 3-1 in Table 1). Using this program, the ionization filament was first heated to 2.8 A at a rate of 0.56 A/min. Then, the evaporation filament was heated to 0.5 A at a rate of 0.1 A/min. After the ionization and evaporation filaments reached 2.8 A and 0.5 A, the current of the evaporation filament was increased at a rate of 0.05 A/min until the beam intensity of the pilot mass reached 5 mV. The highest abundance isotope peak was chosen for the pilot monitor mass to avoid excess heating during lens tuning. We avoided ^{138}Ba owing to its extremely high abundance. Instead, ^{137}Ba was used for unspiked runs and ^{135}Ba was used for spiked and mixture runs because ^{135}Ba had the highest abundance in the latter samples. The ion lenses were then optimized to focus 1 min later. The electric current of the evaporation filament was increased again at a rate of 0.05 A/min until the beam intensity of the pilot mass reached 10 mV. Peak centering was performed 1 min later, and the data acquisition was started. During data acquisition, the electric current of the evaporation filament was increased at ~5 mA/cycle unless the pilot beam intensity exceeded 4200 mV. The integration time was 1.05 s/cycle. The data acquisition was terminated when the pilot beam intensity decayed below 5 mV, which was set as the noise threshold. The raw beam intensity data of all cycles were

Table 1. Combination of the method files for fully automated DS-TEV-TIMS measurement for one sample on the filament, modified from Miyazaki et al. (2009).

Method File	Operation	Acquired data	Time
1	Gain calibration	Gain data (stored in operating computer)	≈ 15 min
2	Baseline measurement	Baseline data (stored in operating computer)	≈ 15 min
3-1	Filament heating (Until pilot beam reach 10 mV), Focusing, and peak centering		≈ 15 min
3-2	Sample measurement by TEV	Raw intensity data of sample (used for off-line calculation)	Max 35 min
4	Blank measurement for baseline drift correction	Raw intensity data without ion beam (used for off-line calculation)	≈ 15 min

summed for each isotope; these summed intensities were used to calculate the isotope ratios.

In this study, we assumed that the MDF followed an exponential law. The three-dimensional data reduction procedure of Siebert et al. (2001) was applied. The $^{134}Ba/^{130}Ba$, $^{135}Ba/^{130}Ba$, and $^{137}Ba/^{130}Ba$ ratios determined by using the summed intensity data were used for regression calculations in an Excel spreadsheet to obtain the corrected $^{134}Ba/^{130}Ba$, $^{135}Ba/^{130}Ba$, and $^{137}Ba/^{130}Ba$ ratios by the DS method. For the regression calculations, the measured isotope ratios of the unspiked sample (standard in this study) and the DS-spiked sample were used. The $^{137}Ba/^{134}Ba$ ratio was calculated to determine the $\delta^{137/134}Ba$ value based on the following equation: $\delta^{137/134}Ba = [(^{137}Ba/^{134}Ba_{sample})/(^{137}Ba/^{134}Ba_{standard})\text{-}1] \times 1000$. The strong ^{138}Ba signal (71.7% isotopic abundance) was not measured in this study to avoid any damage of the designated Faraday cup, although $\delta^{138/134}Ba$ has been used in many studies. The $\delta^{138/134}Ba$ value can be calculated from the $\delta^{137/134}Ba$ value when MIF is not present in the analyzed samples.

The tailing of the strongest ^{138}Ba signal (no Faraday cup assignment) was not detected by the neighboring higher mass side Faraday cup (High 3: ^{139}La). The mass peaks show totally symmetry shape by the TIMS, tailing from ^{138}Ba on the low mass side Faraday (High 2: ^{137}Ba) should also be negligible.

3. DS calibration

3.1 DS calibration methods in previous studies

For high-precision DS isotope analysis with minimized propagated errors, optimized conditions such as the choice of isotopes and mixing ratio of two spikes were simulated by the model proposed by Rudge et al. (2009). We applied ^{130}Ba and ^{135}Ba as the DS spikes and prepared a ^{130}Ba–^{135}Ba DS solution based on the simulation. The isotope ratios used for the ^{130}Ba–^{135}Ba DS were calculated from the weight and atomic abundance data supplied by the ORNL, where $^{134}Ba/^{130}Ba = 0.076432$, $^{135}Ba/^{130}Ba = 1.040925$, and $^{137}Ba/^{130}Ba = 0.208963$ (Table 2). Notably, small but inevitable errors that occur during weighing and diluting as well as additional errors are inherited from ORNL reference atomic abundance values, all of which affect the isotope ratios of the ^{130}Ba–^{135}Ba DS solution. Therefore, calibration is required to determine accurate isotope ratios of the DS solution. In the case of stable Ba isotopes, such calibration is difficult owing to the lack of a standard material with well-characterized isotope ratios (Miyazaki et al., 2014).

Several calibration methods can be used to overcome the aforementioned problem. For example, von Allmen et al. (2010) and van Zuilen et al. (2016) calibrated their ^{130}Ba–^{135}Ba DS solution by applying the fractionation factor of the $^{142}Nd/^{144}Nd$ ratio of an Nd standard to their analytical protocols using MC-ICP-MS. This external mass fractionation calibration is not applicable to TIMS because the evaporation and ionization conditions for Ba and Nd differ such that emission of stable ion beams under a given filament temperature is difficult. Even with MC-ICP-MS, the mass bias determined by using the $^{142}Nd/^{144}Nd$ ratio is different from that based on the $^{137}Ba/^{135}Ba$ ratio because of the space charge effect at the ion sampling interface (Hirata, 1996) or non-mass-dependent fractionation of Nd isotopes (Newman, 2012), as pointed out by Miyazaki et al. (2014).

Therefore, Miyazaki et al. (2014) developed a new DS calibration method that does not depend on the use of standard material with well-known isotope ratios. They revealed that a precise Ba isotope ratio measurement can be achieved only by using the correct DS isotope ratios when unknown samples with different spike/sample ratios are measured with the standard bracketing method and MC-ICP-MS. They conducted several measurements using IAEA-CO-9 with different spike/sample ratios (0.11–0.33) as the samples and IAEA-CO-9 with a fixed spike/standard ratio (0.175) as the bracketing standard, and they iteratively determined the correct ^{130}Ba–^{135}Ba DS isotope ratios to achieve an invariant value for all measured $\delta^{137/134}Ba$ values. The initial assumption of their calibration method is that the true DS isotope ratio plots on the mixing line of the two spikes.

Van Zuilen et al. (2016) also reported a DS calibration method using TIMS in which they calibrated ^{132}Ba–^{136}Ba DS, also without using material with known isotope ratios. In contrast to the mixing line method by Miyazaki et al. (2014), they measured the pure DS solution and artificially altered the DS Ba isotope ratios along the MDF line using an exponential law to determine the average values of $\delta^{137/134}Ba$ and $\delta^{138/134}Ba$ of the target NIST SRM 3104a becoming 0‰.

In this study, we adopted both the mixing line

method of Miyazaki et al. (2014) and the MDF line method of van Zuilen et al. (2016), and we used TEV-TIMS to calibrate the ^{130}Ba–^{135}Ba DS solution.

Table 2. Double-spike data used in this study.

	Data supplied by ORNL		Recalculated as 100%		Mixing ratio (0.746)		TE-TIMS	Mixing line method
	^{130}Ba Spike	^{135}Ba Spike	^{130}Ba Spike	^{135}Ba Spike	Estimated DS		Measured DS	Corrected DS
^{130}Ba (%)	35.84 ± 0.007	<0.01	35.84	0.01	26.75			
^{132}Ba (%)	0.41 ± 0.001	0.06 ± 0.005	0.41	0.06	0.32			
^{134}Ba (%)	2.58 ± 0.001	0.47 ± 0.005	2.58	0.47	2.04			
^{135}Ba (%)	5.55 ± 0.011	93.38 ± 0.02	5.55	93.38	27.84			
^{136}Ba (%)	5.56 ± 0.001	1.64 ± 0.01	5.56	1.64	4.56			
^{137}Ba (%)	7.19 ± 0.001	0.89 ± 0.01	7.19	0.89	5.59			
^{138}Ba (%)	42.88 ± 0.002	3.56 ± 0.02	42.88	3.56	32.90			
^{134}Ba/^{130}Ba						Run 1	0.077115	0.076621
						Run 2	0.077027	0.076624
						Run 3	0.077025	0.076624
						Run 4	0.076977	0.076624
						Run 5	0.077043	0.076622
						Run 6	0.077278	0.076623
						Run 7	0.077135	0.076623
						Run 8	0.077028	0.076624
						Run 9	0.077203	0.076623
						Run 10	0.077009	0.076624
						Run 11	0.077011	0.076622
						Run 12	0.077051	0.076624
			0.072017	46.60	0.076432	Average	0.077075	0.076623
						2SD (n = 12)	0.000180	0.000002
^{135}Ba/^{130}Ba						Run 1	1.091073	1.082089
						Run 2	1.089266	1.081960
						Run 3	1.089238	1.081951
						Run 4	1.088430	1.081989
						Run 5	1.089636	1.081965
						Run 6	1.093857	1.082065
						Run 7	1.091180	1.081917
						Run 8	1.089278	1.081960
						Run 9	1.092384	1.081931
						Run 10	1.088962	1.081962
						Run 11	1.089051	1.081955
						Run 12	1.089699	1.081954
			0.154776	9338	1.040925	Average	1.090171	1.081975
						2SD (n = 12)	0.003250	0.000102
^{137}Ba/^{130}Ba						Run 1	0.211780	0.209357
						Run 2	0.211325	0.209355
						Run 3	0.211320	0.209355
						Run 4	0.211092	0.209356
						Run 5	0.211424	0.209356
						Run 6	0.212537	0.209357
						Run 7	0.211853	0.209355
						Run 8	0.211328	0.209355
						Run 9	0.212174	0.209355
						Run 10	0.211243	0.209355
						Run 11	0.211269	0.209356
						Run 12	0.211443	0.209355
			0.200536	89.00	0.208963	Average	0.211566	0.209356
						2SD (n = 12)	0.000867	0.000001

DS: ^{130}Ba–^{135}Ba double spike, SD: standard deviation.

3.2 DS calibration methods by TEV-TIMS

The isotope ratio measurements in TEV-TIMS is almost free from the influence of MDF owing to the acquisition of all ions emitted from the sample on the filament (e.g., Suzuki et al., 2004; Fukami et al., 2017). Therefore, TEV-TIMS is suitable for precise determination of isotope ratios of any DS solution. However, the actual measurements of the ^{130}Ba–^{135}Ba DS solution by TEV-TIMS showed MDF (Table 2, Fig. 1), whereas significant MIF was not observed. As shown in Fig. 1, all data points were on the MDF line. The origin of MDF is unknown and may be attributed to MDF occurrence during sample loading or filament heating. Alternatively, it may have been caused by the effect of the noise threshold cutoff or the collision of ions with remnant gases in the flight tube. Regardless of its source, however, additional MDF correction is necessary.

If the measured isotope ratios of the DS solution are affected by MDF alone, the MDF line calculated from the datapoints should cross the mixing line between the two spikes, and the coordinates of the intercept should show the correct isotope ratios of the DS solution (Fig. 1). However, the calculated MDF did not cross at the exact coordinates in three two-dimensional isotope spaces (Fig. 1). This result occurred because of the correlation errors in MDF regression lines and the mixing line owing to a common denominator with three numerator isotopes such as ^{137}Ba/^{130}Ba–^{135}Ba/^{130}Ba, ^{134}Ba/^{130}Ba–^{135}Ba/^{130}Ba, or ^{137}Ba/^{130}Ba–^{134}Ba/^{130}Ba (Fig. 1). Instead of determining each intercept coordinates by linear regressions using all data, we iteratively determined the best fit solutions for each measured isotope MDF data. We applied an Excel spreadsheet and calculated 12 intercept values for ^{134}Ba/^{130}Ba, ^{135}Ba/^{130}Ba, and ^{137}Ba/^{130}Ba, which were averaged to obtain the isotope ratios of the spike solution. Using this method, we calibrated the ^{130}Ba–^{135}Ba DS solution. The calibrated isotope ratios were ^{134}Ba/^{130}Ba = 0.076623 ± 0.000002, ^{135}Ba/^{130}Ba = 1.081975 ± 0.000102, and ^{137}Ba/^{130}Ba = 0.209356 ± 0.000001 (2SD: two-standard deviation, n = 12) (Table 2, Fig. 1).

The errors of the atomic abundances provided by the ORNL for the two spikes were not considered. We used a fixed line as mixing line; therefore, it was necessary to estimate the degree to which the calibrated isotope ratios were influenced by the initial errors of the atomic abundances listed in Table 2. We simply estimated the effects of the errors by applying the maximum and minimum atomic abundances of the error ranges. The maximum effect is shown by ^{135}Ba/^{130}Ba = 1.081233–1.082718, corresponding to an error of ± 686 ppm. According to the simulation by Miyazaki et al. (2014), the atomic abundance error of ± 686 ppm (^{135}Ba/^{130}Ba ratio of spike) affects the $\delta^{137/134}$Ba values within ± 0.01‰ for measurements using a spike/sample ratio

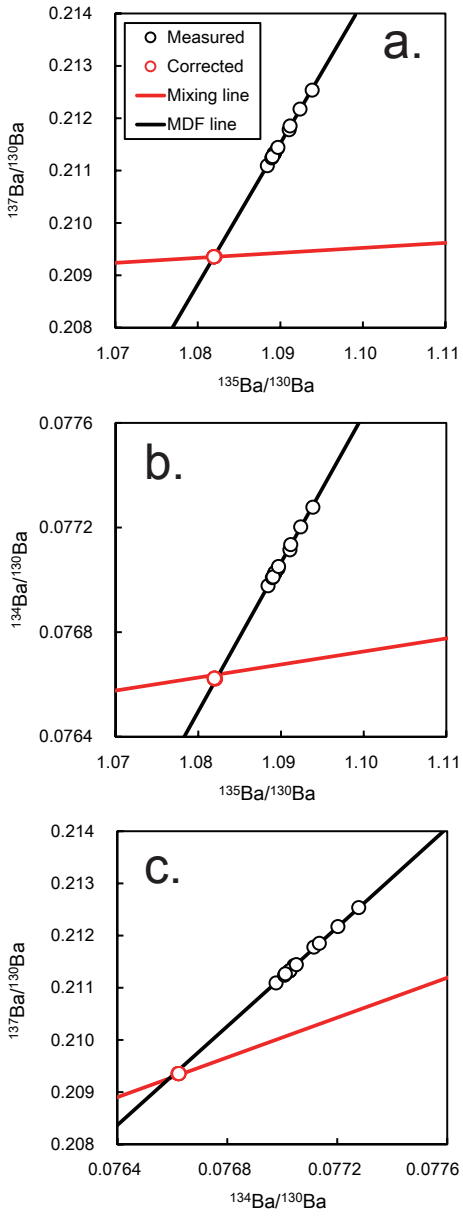

Fig. 1. Relationship between the measured and corrected isotope ratios of spikes in the three isotope-ratio space (^{134}Ba/^{130}Ba–^{135}Ba/^{130}Ba–^{137}Ba/^{130}Ba) shown by three projected planes. The open black (red) circles represent the measured (corrected) spike data listed in Table 2. The black line shows the MDF line calculated from the average measured data. The red line represents the mixing line drawn between the ^{130}Ba- and ^{135}Ba-enriched spikes. (a) ^{135}Ba/^{130}Ba–^{137}Ba/^{130}Ba plot; (b) ^{135}Ba/^{130}Ba–^{134}Ba/^{130}Ba plot; (c) ^{134}Ba/^{130}Ba–^{137}Ba/^{130}Ba plot.

of 0.03–0.28 in sample run if the spike/standard ratio of the bracketing mixture is fixed to 0.178. The resultant error is smaller than the achievable repeatability and laboratory biases of ~ 0.02‰ for stable Ba isotope analyses (Miyazaki et al., 2014). Therefore, we ignored the atomic abundance errors of the two ORNL spikes in this study.

4. Stable Ba isotope analysis of NIST SRM 3104a

To evaluate the TEV-DS-TIMS method for determining the stable Ba isotope ratios, we analyzed NIST standard SRM 3104a. The typical profiles of the ^{135}Ba beam signal intensity and the electric current of the evaporation filament are shown in Fig. 2a. The beam intensity increased rapidly and was maintained at the preset intensity of 4200 mV. The increment of the filament current was automatically adjusted to maintain the preset beam intensity. Subsequently, the intensity rapidly decreased and rose again, leading to two peaks showing aftergrowth. The beam intensity finally returned to zero, indicating full consumption of the loaded sample. Aftergrowth was observed in almost all measurements conducted in this study. The first drop in beam intensity prior to aftergrowth commonly occurred when the electric current of the evaporation filament was 1.0–1.5 A. Although the cause of this reproducible profile is unclear, it might not relate to differences in chemical form, such as the nitric or hydrochloric form, because all Ba standard and spike solutions were diluted by nitric acid only. For further evaluation, the signal profile was divided into four segments of A, B, C, and D (Fig. 2) at 0.155 V intensity. It should be noted that this value corresponds with the lowest intensity between the first drop and the aftergrowth (Fig. 2).

Fig. 3 shows the plots of the ^{137}Ba/^{130}Ba and ^{135}Ba/^{130}Ba ratios from all 1060 cycles of 1.05 s acquisition in one measurement; Fig. 2 shows the same sample. Although the data from the first A (lighter isotope ratio) and last D (heavier isotope ratio) segments were scattered because of the low beam intensity, all of the other data including the B and C segments were plotted along the MDF line. Therefore, the scatter data in the A and D segments can be omitted by applying the threshold. It is obvious that all Ba ions emitted from the evaporation filament were derived from the same sample throughout the run. The effect of Ba impurity emitted from the degassed Re filaments was negligible because only 12000 cps of ^{138}Ba, an equivalent of

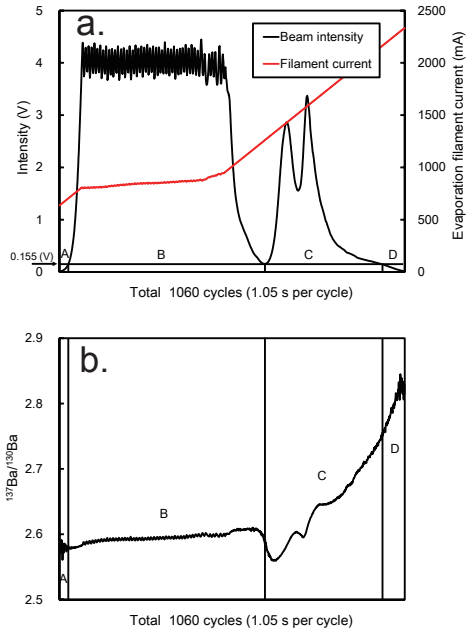

Fig. 2. (a) Intensity profiles of the ^{135}Ba beam signal intensity and electric current loaded onto the evaporation filament for measurement of the spiked solution. A total of 100 ng of Ba (NIST SRM 3104a + ^{130}Ba–^{135}Ba double spike) was loaded onto the evaporation filament. The electric current of the ionization filament was fixed at 2.8 A. The profile is divided into four segments of A, B, C, and D at intensity 0.155 V; this value is the lowest intensity between the first drop and the aftergrowth. (b) ^{137}Ba/^{130}Ba ratios of 1060 cycles of individual 1.05 s acquisitions in one measurement run.

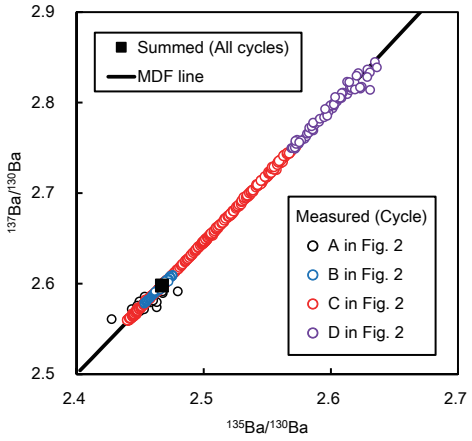

Fig. 3. ^{135}Ba/^{130}Ba–^{137}Ba/^{130}Ba plots of 1060 cycles of individual 1.05 s acquisitions in one measurement run. The cycles accumulated in the four divided segments in Fig. 2 are distinguished by different colors. The measured sample contained 100 ng of Ba (NIST SRM 3104a + ^{130}Ba–^{135}Ba double spike); the same sample was used in Fig. 2. The black filled square and the black line represent the calculated isotope ratios and the MDF line from the summed values of all cycle data, respectively.

<0.2 mV in the Faraday collector, was detected at filament currents of 4.2 A for ionization and ~2.5 A for evaporation.

The range of fractionation observed in segment C was wide and overlapped the range of the B segment. Lower isotope ratios relative to those in segment B were found in segment C, showing so-called reverse fractionation (Fig. 2b, Fig. 3) caused by ion mixing fed from strongly fractionated and weakly fractionated reservoirs on the same filament (Upadhyay et al., 2008; Andreasen and Sharma, 2009). Essentially, the data from the reverse fractionation region might not be shown on the MDF line but could appear on the mixing line between the two less- and more-fractionated reservoirs, although the data from the reverse fractionation region looks on the same MDF line (Fig. 3). Applying the total evaporation method can eliminate the non-MDF effect from the reverse fractionation if persistent.

Table 3 and Fig. 4 show the results of the measurements of the NIST SRM 3104a standard solution by TEV-TIMS with and without DS correction. Following

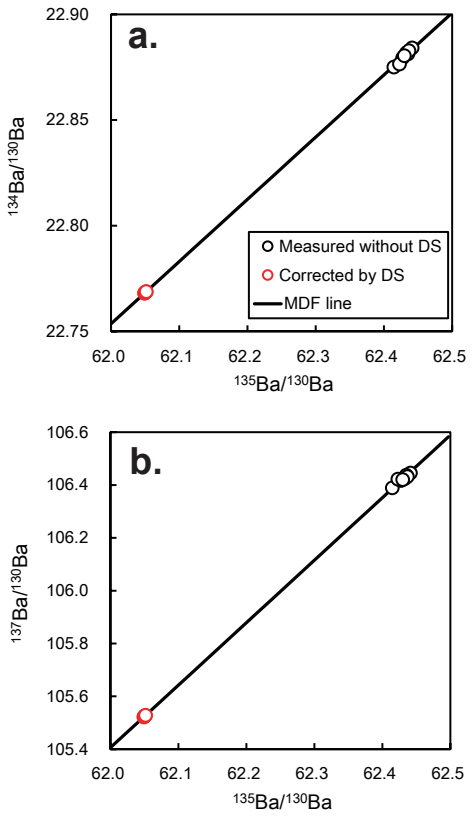

Fig. 4. Comparisons of the data from NIST SRM 3104a determined with and without using double-spike corrections based on the ^{130}Ba–^{135}Ba double spike. The black line shows the MDF line calculated from the average values of the measured data without DS. Seven red points (corrected by DS) overlap owing to small isotopic variation. (a) ^{135}Ba/^{130}Ba–^{134}Ba/^{130}Ba plot. (b) ^{135}Ba/^{130}Ba–^{137}Ba/^{130}Ba plot.

simulations by Rudge et al. (2009) and Miyazaki et al. (2014), a spike/standard ratio of 0.175 was applied to prepare the mixed solution to minimize errors. The average isotope ratios of the unspiked runs (^{134}Ba/^{130}Ba = 22.8802, ^{135}Ba/^{130}Ba = 62.4301, and ^{137}Ba/^{130}Ba = 106.4235) were used as the sample ratios of an unspiked run to calculate the corrected isotope ratios of each spiked run. If the Ba isotope ratios of sample are affected only by MDF, correction is possible by using a spiked run only (mixture run only). In this case, an optimal MDF factor should have been determined. We used Ba isotope ratios determined by an unspiked NIST SRM 3104a to obtain the optimal MDF factor. As expected, the isotope ratios from DS correction showed lower isotope ratios (Fig. 4) with smaller deviation than those from measurements without DS correction. If we calculate the errors of the δ-notation using the average ^{137}Ba/^{134}Ba ratios from DS correction as reference values, the deviations of the $\delta^{137/134}$Ba values are ± 0.018‰ (2SD, n = 7) for DS-corrected and ± 0.165‰ (2SD, n = 8) for uncorrected results, where 2SD contains error ranges of ± 0.001‰ and ± 0.012‰, respectively, owing to the small value of n. Clearly, the repeatability of $\delta^{137/134}$Ba is far better using DS correction and is comparable to or even better than that of the best values reported in previous studies. For example, Miyazaki et al. (2014) reported ± 0.032‰ (2SD, n = 42) for $\delta^{137/134}$Ba of the Fluka (Aldrich) standard solution, and Nan et al. (2015) reported ± 0.047‰ (2SD, n = 36) for $\delta^{137/134}$Ba of the NIST SRM 3104a standard solution.

The isotope ratios for NIST SRM 3104a (Lot No. 070222) are only available from van Zuilen et al. (2016) (Table 3). Their isotope ratios differ from ours beyond the variation observed in natural samples (e.g., seawater; Cao et al., 2016). A comparison based on our NIST SRM 3104a ratio as reference revealed that their $\delta^{137/134}$Ba value is 1.723‰. Such large variation was observed only in the experimental study by van Zuilen et al. (2016), who reported a maximum difference of 2.15‰ for $\delta^{137/134}$Ba owing to diffusion. This clearly indicates the importance of an international, isotopically homogeneous Ba reference material for the δ-notation. The NIST SRM 3104a standard has been proposed as δ-zero reference material for stable Ba isotope analysis (van Zuilen et al., 2016). However, the same NIST SRM 3104a standard (Lot No. 140909) used in this study was newly released in February 2016. Its certified Ba concentration differs from that of the previous lot, with 10.014 ± 0.036 mg/g for Lot No. 070222 (van Zuilen et al.,

2016) versus 6.994 ± 0.0017 mg/g for Lot No. 140909 used in this study. At this stage, it is not clear that the different $\delta^{137/134}$Ba values reported from van Zuilen et al. (2016) were caused by different analytical method because the standard from a different production lot could have different Ba isotope composition. In fact, NIST SRM 3104a is not the standard for Ba isotope ratios but for Ba concentration, as van Zuilen et al. (2016) suggested the necessity of tests for different lots of NIST SRM 3104a.

5. Conclusion

We developed a precise analytical method for determining stable Ba isotope ratios using DS-TEV-TIMS. In this method, the DS was used for MDF correction in the TIMS instrument. The DS solution created from ORNL spikes was calibrated without using a Ba standard by instead determining the relationship between the MDF lines of the DS solution and the mixing lines between the two Ba spikes. The repeatability of the $\delta^{137/134}$Ba ratios based on repeated analyses of a standard solution was approximately twice that reported in previous studies.

Table 3. Result of Ba isotope analysis for NIST SRM 3104a (Lot No. 140909).

Run #	^{134}Ba/^{130}Ba	^{135}Ba/^{130}Ba	^{137}Ba/^{130}Ba	^{137}Ba/^{134}Ba	$\delta^{137/134}$Ba[a]
a. Measured ratios of NIST SRM 3104a without double-spike					
1	22.8751	62.4146	106.3892	4.65088	3.328
2	22.8818	62.4331	106.4245	4.65105	3.363
3	22.8794	62.4274	106.4170	4.65121	3.398
4	22.8765	62.4227	106.4224	4.65204	3.577
5	22.8841	62.4413	106.4454	4.65149	3.459
6	22.8813	62.4351	106.4372	4.65172	3.508
7	22.8828	62.4367	106.4320	4.65118	3.392
8	22.8805	62.4300	106.4206	4.65116	3.387
Average	22.8802	62.4301	106.4235	4.65134	3.426
2SD (n=8)	0.0062	0.0170	0.0335	0.00076	0.165
b. Measured ratios of mixture (NIST SRM 3104a + ^{130}Ba − ^{135}Ba double spike)					
1	0.589315	2.467152	2.597872		
2	0.589242	2.466804	2.597372		
3	0.589167	2.466396	2.596771		
4	0.589102	2.466031	2.596217		
5	0.589286	2.466970	2.597596		
6	0.589167	2.466384	2.596742		
7	0.589137	2.466236	2.596551		
Average	0.589202	2.466567	2.597017		
2SD (n=7)	0.000160	0.000825	0.001207		
c. Corrected ratios of NIST SRM 3104a calculated from b					
1	22.7684	62.0503	105.5248	4.63471	−0.001
2	22.7687	62.0514	105.5274	4.63476	0.010
3	22.7686	62.0509	105.5262	4.63473	0.005
4	22.7681	62.0493	105.5225	4.63467	−0.010
5	22.7681	62.0492	105.5222	4.63466	−0.011
6	22.7683	62.0500	105.5241	4.63470	−0.004
7	22.7688	62.0517	105.5280	4.63477	0.012
Average	22.7684	62.0504	105.5250	4.63471	0.000
2SD (n=7)	0.0006	0.0019	0.0046	0.00008	0.018
d. NIST SRM 3104a (Lot No. 070222) in van Zuilen et al. (2016)					
	22.7998	62.1762	105.8527	4.64270	1.723

[a] The average ^{137}Ba/^{134}Ba ratio of corrected ratio of NIST SRM 3104a (4.63471) is used as standard ratio.

Acknowledgements

The authors thank W. Zhang, H. Higuchi, and M. Kanazawa of JAMSTEC for their support with the laboratory work and Q. Chang for useful discussion. In addition, the authors thank two anonymous reviewers for their constructive comments and H. Kumagai for his constructive comments and editorial handling. T.M. was funded by a JSPS KAKENHI grant JP15K05357.

References

Andreasen, R. and M. Sharma (2009), Fractionation and mixing in a thermal ionization mass spectrometer source: Implications and limitations for high-precision Nd isotope analyses, *Int. J. Mass Spectrom.*, *285*, 49–57, doi:10.1016/j.ijms.2009.04.004.

Cao, Z., C. Siebert, E.C. Hathorne, M. Dai, and M. Frank (2016), Constraining the oceanic barium cycle with stable barium isotopes, *Earth Planet. Sci. Lett.*, *434*, 1–9, doi:/10.1016/j.epsl.2015.11.017.

de Laeter, J.R., J.K. Böhlke, P. De Bièvre, H. Hidaka, H.S. Peiser, K.J.R. Rosman, and P.D.P. Taylor (2003), Atomic weights of the elements. Review 2000 (IUPAC Technical Report), *Pure Appl. Chem.*, *75*, 683–800, doi: 10.1351/pac200375060683.

Fukami, Y., M. Tobita, T. Yokoyama, T. Usui, and R. Moriwaki (2017), Precise isotope analysis of sub-nanogram lead by total evaporation thermal ionization mass spectrometry (TE-TIMS) coupled with a ^{204}Pb-^{207}Pb double spike method, *J. Anal. At. Spectrom.*, *32*, 848–857, doi:10.1039/C6JA00455E.

Hirata, T. (1996), Lead isotope analyses of NIST Standard Reference Materials using multiple collector inductively coupled plasma mass spectrometry coupled with a modified external correction method for mass discrimination effect, *Analyst*, *121*, 1407–1411, doi:10.1039/AN9962101407.

Lu, D., T. Zhang, X. Yang, P. Su, Q. Liu, and G. Jiang (2017), Recent advances in the analysis of non-traditional stable isotopes by multi-collector inductively coupled plasma mass spectrometry, *J. Anal. At. Spectrom.*, *32*, 1848–1861, doi:10.1039/C7JA00260B.

Miyazaki, T., N. Kanazawa, T. Takahashi, Y. Hirahara, B.S. Vaglarov, Q. Chang, J.-I. Kimura, and Y. Tatsumi (2009), Precise Pb isotope analysis of igneous rocks using fully-automated double spike thermal ionization mass spectrometry (FA -DS- TIMS), *JAMSTEC Rep. Res. Dev.*, Special Issue, 73–80, doi:10.5918/jamstecr.2009.73

Miyazaki, T., J.-I. Kimura, and Q. Chang (2014), Analysis of stable isotope ratios of Ba by double-spike standard-sample bracketing using multiple-collector inductively coupled plasma mass spectrometry, *J. Anal. At. Spectrom.*, *29*, 483–490, doi:10.1039/c3ja50311a.

Miyazaki, T., B.S. Vaglarov, and J.-I. Kimura (2016), Determination of relative Faraday cup efficiency factor using exponential law mass fractionation model for multiple collector thermal ionization mass spectrometry, *Geochem. J.*, *50*, 445–447, doi:10.2343/geochemj.2.0439.

Nan, X., F. Wu, Z. Zhang, Z. Hou, F. Huang, and H. Yu (2015), High-precision barium isotope measurements by MC-ICP-MS, *J. Anal. At. Spectrom.*, *30*, 2307–2315, doi:10.1039/C5JA00166H.

Newman, K. (2012), Effects of the sampling interface in MC-ICP-MS: Relative elemental sensitivities and non-linear mass dependent fractionation of Nd isotopes, *J. Anal. At. Spectrom.*, *27*, 63–70, doi:10.1039/C1JA10222B.

Rudge, J.F., B.C. Reynolds, and B. Bourdon (2009), The double spike toolbox, *Chem. Geol.*, *265*, 420–431, doi:10.1016/j.chemgeo.2009.05.010.

Siebert, C., T.F. Nägler, and J.D. Kramers (2001), Determination of molybdenum isotope fractionation by double-spike multicollector inductively coupled plasma mass spectrometry, *Geochem., Geophys., Geosyst.*, *2*, 2000GC00124, doi:10.1029/2000GC000124.

Suzuki, K., Y. Miyata, and N. Kanazawa (2004), Precise Re isotope ratio measurements by negative thermal ionization mass spectrometry (NTI-MS) using total evaporation technique, *Int. J. Mass Spectrom.*, *235*, 97–101, doi:10.1016/j.ijms.2004.04.006.

Upadhyay, D., E.E. Scherer, and K. Mezger (2008), Fractionation and mixing of Nd isotopes during thermal ionization mass spectrometry: implications for high precision ^{142}Nd/^{144}Nd analyses, *J. Anal. At. Spectrom.*, *23*, 561–568, doi:10.1039/B715585A.

van Zuilen, K., T.F. Nägler, and T.D. Bullen (2016), Barium Isotope Compositions of Geological Reference Materials, *Geostand. Geoanal. Res.*, *40*, 543–558, doi:10.1111/ggr.12122.

von Allmen, K., M.E. Böttcher, E. Samankassou, and T.F. Nägler (2010), Barium isotope fractionation in the global barium cycle: First evidence from barium minerals and precipitation experiments, *Chem. Geol.*, *277*, 70–77, doi:10.1016/j.chemgeo.2010.07.011.